Evaluation of the Capability of Landsat 7/ETM+ Imagery for Damage Detection due to 2001 Atico, Peru Earthquake

The University of Tokyo, Institute of Industrial Science — Student Member — Miguel ESTRADA
The University of Tokyo, Institute of Industrial Science — Member — Masayuki KOHIYAMA
Asian Institute of Technology — Member — Fumio YAMAZAKI

Introduction. For the evaluation of damage after a natural disaster occurs different methods exist. As a result of the progress and advances in remote sensing technologies as well as information that may be readily obtained from civilian satellites, satellite imagery is gaining acceptation nowadays for damage detection. In this paper the capability of Landsat 7/ETM+ imagery to evaluate the damage caused by the 2001 Atico, Peru earthquake is assessed.

Data and Methodology. The study area is the city of Moquegua located in southern Peru (1,144 km from Lima, the capital city, see Figure 1). Moquegua was one of the most heavily affected cities caused by the earthquake due to the concentration of adobe houses. Change detection techniques for remotely sensed images are based on applying specialized algorithm to two satellite images of the same area acquired at different times. In this study Landsat 7/ETM+ images taken before and after the event have been used to study the effects of the earthquake. The pre-event set was acquired on May 26, 2001, 28 days before the earthquake, while the post-event set was taken on June 27, 2001, 4 days after the event (Figure 2). A digital map of Moquegua City at scale 1:25,000 is also available. Some statistical information about the damage in different sectors of Moquegua City was kindly provided by CISMID[1].

At first pre-processing of images was carried out. It considers atmospheric correction (regression method[2]), geo-graphic correction (image-to-map registration), integration of a digital map with the remote sensing images and image enhancement (HSI transformation[3]).

The assessment of the use of satellite imagery was carried out by comparing the results of three methods for damage detection. The first method is computation of the ratio of the normalized difference indices of the post- and pre-event images. The second method is the image correlation analysis between the enhanced pre- and post-event images. The third method is the use of the principal component transformation, applied to a 12-bands set obtained by combining all non-thermal bands of the pre- and post-event images.

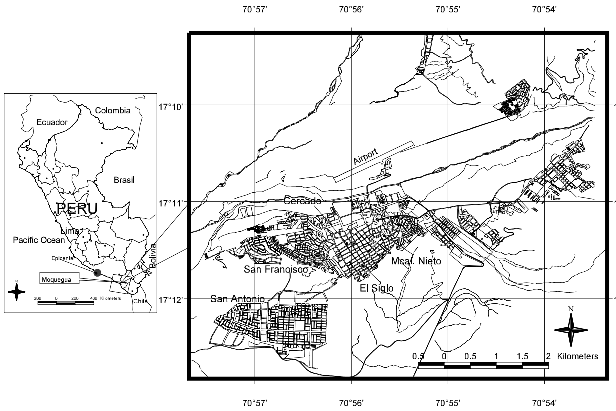

Figure 1. Map of the study area. Moquegua City.

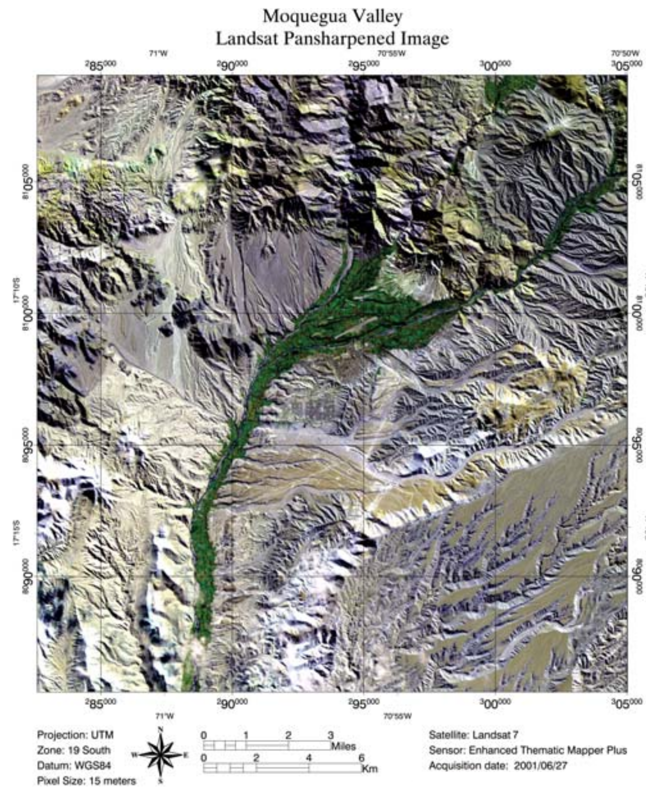

Figure 2. Pansharpened Landsat image of Moquegua

Normalized ratios. Based on the basic idea of the NDVI other normalized indices can be obtained by combining the different bands in the visible range of the spectrum. In this paper three kinds of normalized indices have been used based on the first three bands of the image set, they are:

$$R1 = (B1 - B2)/(B1 + B2),$$
$$R2 = (B1 - B3)/(B1 + B3), \text{ and} \qquad (1)$$
$$R3 = (B2 - B3)/(B2 + B3)$$

where $B1$, $B2$, and $B3$ are the pixel values of band 1, 2 and 3, respectively. Once these three normalized ratios have been obtained for the pre- and post-event images, the following second ratios are computed to see if changes can be detected:

$$SR1 = R1_{after} / R1_{before},$$
$$SR2 = R2_{after} / R2_{before}, \text{ and} \qquad (2)$$
$$SR3 = R3_{after} / R3_{before}$$

The mean values and standard deviations of ratio R3 of five sectors in Moquegua City are shown in Figure 3. The sectors are ordered by their levels of damage, from major to minor damage. As it can be seen, for higher level of damage the ratio SR3 is greater than 1 and descends along with the lower level of damage. Although a tendency can be observed in the values

Key words: The 2001 Atico-Peru earthquake, damage detection, Landsat 7/ETM+, image correlation, image enhancement.
Contact Address: Bw304, 4-6-1 Komaba, Meguro-ku, Tokyo 153-8505, Tel. (+81) 3-5452-6388, Fax (+81) 3-5452-6389.

of the ratio SR3, it should be noticed that the standard deviations are considerably large.

Image Correlation Analysis. Correlation analysis is the statistical tool that can be used to describe the degree to which two variables are "correlated" to each other. Is very common to use correlation analysis for automated detection of ground control points and thus conduct the image-to-image registration[3]. However, correlation analysis can also be used to measure the degree of relationship between two variables. From the correlation indices between the pre- and post-event images, new images are generated called correlation images. A square-shape moving window of size *ws* (being *ws* an odd number) is moved pixel by pixel and in each position (m, n) the correlation index is calculated, and thus generating the corresponding new pixel value for the correlation image. The correlation index was calculated for each one of the bands of the pre- and post-event enhanced images bands red, green and blue. The moving window's sizes, 3x3 pixels, 5x5 pixels and 7x7 pixels were utilized. The used correlation coefficient is given by:

$$r_{mn} = \left(\sum_{j=1}^{ws} \sum_{i=1}^{ws} a_{ij} b_{ij} \right)^2 \Bigg/ \sum_{j=1}^{ws} \sum_{i=1}^{ws} a_{ij}^2 \sum_{j=1}^{ws} \sum_{i=1}^{ws} b_{ij}^2 \tag{3}$$

where r_{mn}=correlation coefficient of the (m, n) position of the moving window, a_{ij}= digital number of the (i, j) pixel of the post-event image, and b_{ij}= digital number of the (i, j) pixel of the pre-event image.

As it was expected, lower values of correlation indicate high level of damage whereas values near the unit belong to the zones of minor damage (Figure 4). The three moving windows gave similar results.

Principal Component Analysis (PCA). The purpose of the PCA is to compress all of the information contained in an original *n*-bands data set into fewer *m* new bands or *components;* it reduces the redundancy in multispectral data. Let $L=\{L_1(DN_k), L_2(DN_k)\}$ be a combined set of $2n$ bands images composed of two different dates images and C_L be the variance-covariance matrix of L. Each principal component X_j is expressed as:

$$X_j = \sum_{k=1}^{n} \alpha_k L_1(DN_k) + \sum_{k=1}^{n} \beta_k L_2(DN_k) \tag{4}$$

where $\{\alpha_k, \beta_k\}$ is the normalized eigenvectors of the variance-covariance matrix C_L of L. Difference of the surface reflectance between two dates is evaluated by the following principal component:

$$D = \sum_{k=1}^{n} \alpha_k L_1(DN_k) + \sum_{k=1}^{n} \beta_k L_2(DN_k),\ (\alpha_k > 0, \beta_k < 0 \text{ for all } k) \tag{5}$$

In this study the 4th principal component satisfies the condition given by Equation 5, where the first 6 coefficients are positives and the lasts 6 are negative. The mean value and standard deviation of the pixels values of the 4th principal component are shown in Figure 5. As it can be seen, mean values show a tendency from lower values in heavily damage areas increasing along the lower level of damage, however notice that there is a discontinuity in El Siglo sector as well as large values of the standard deviation.

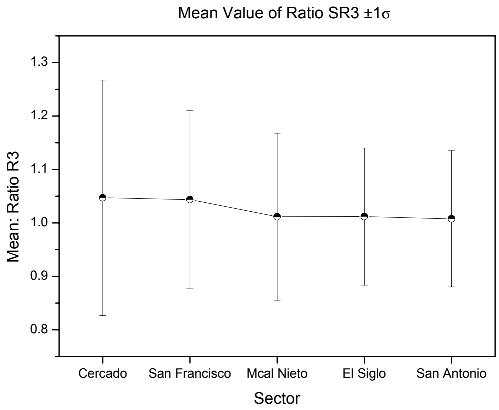

Figure 3. Mean values and standard deviations of ratio SR3. Notice that there is a decreasing trend along with the level of damage, from heavy to minor damage.

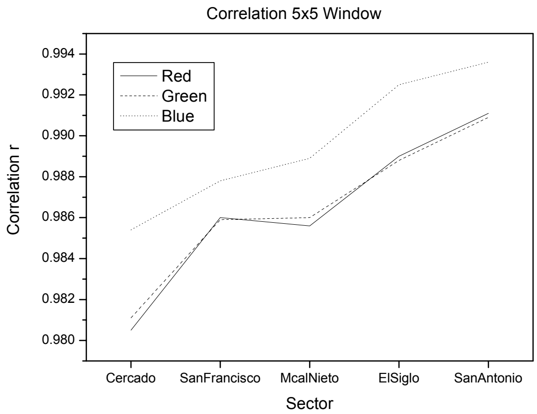

Figure 4. Mean value of the correlation *r* for 5x5 pixels window size.

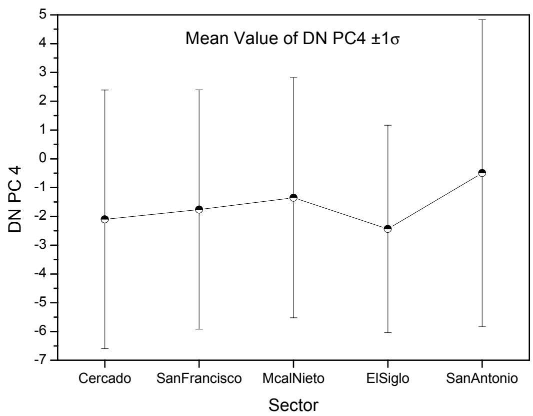

Figure 5. Mean values and standard deviation of the 4th principal component.

Concluding Remarks. For the detection of damage three methods have been applied. For the rationing method, places with high damage showed values greater than 1 and for less damage areas values near to 1. For the correlation method, sectors with high damage showed lower values of correlation while correlation values near to 1 were obtained for minor damage places. In case of principal component analysis, heavy damage sectors showed lower values than less damage areas. In case of this earthquake the clearest tendency has been observed in the image correlation method. However, particularly in this case, due to the large values of the standard deviation there is not a high level of confidence to decide whether a pixel belong a damage area or not.

References

1) Japan-Peru Center for Earthquake Engineering and Disaster Mitigation (CISMID). http://www.cismid.uni.edu.pe
2) Mather, P. M. (1999). Computer Processing of Remotely-Sensed Images: An introduction. Second Ed. John Wiley & Sons Ltd. England.
3) Japan Association on remote Sensing (1996). Remote Sensing Note. Japan Association on Remote Sensing. Japan.